Change in the order of the melting transition with oxygen content in $YBa_2Cu_3O_{7-\delta}$

A. I. Rykov and S. Tajima
Superconductivity Research Laboratory, ISTEC, Tokyo 135-0062, Japan

F. V. Kusmartsev
Department of Physics, Loughborough University, Leicestershire LE11 3TU, United Kingdom and L. D. Landau Institute for Theoretical Physics, Moscow, Russia

E. M. Forgan
School of Physics and Astronomy, University of Birmingham, Birmingham B15 2TT, United Kingdom

Ch. Simon
Laboratoire CRISMAT, ISMRA, 6 Boulevard du Marechal Juin, Caen 14050, France
(Received 11 February 1999; revised manuscript received 24 May 1999)

The vortex phase transition was systematically studied in twin-free $YBa_2Cu_3O_{7-\delta}$ for various δ. For $7-\delta \geqslant 6.94$, the first order transition was evidenced by an abrupt jump and a hysteresis of magnetization in the field-cooled (FC) cooling-warming cycles, which indicates the coexistence of vortex crystallites and liquid. For $7-\delta<6.89$ the jump was not sharp and FC magnetization was reversible, suggesting a second order transition. The first and the second order transitions merge at a critical point (CP) which goes to zero field for $7-\delta<6.89$. Three-dimensional *XY* scaling satisfactorily fits the data at 1–7 T for $7-\delta<6.94$ and for $7-\delta<6.89$, but does not fit for $6.89<7-\delta<6.94$, where the CP passes through this field range.
[S0163-1829(99)14633-2]

I. INTRODUCTION

A subject of general interest in condensed matter is the thermodynamical order of transition from the vortex liquid to the solid. Thermal fluctuations were originally predicted to render the vortex transition first order for space dimensionality $D<6$ and to drive the actual location of the transition far below a mean-field value for $D=2$.[1] In the clean regime of quasi-two-dimensional (2D) layered cuprates, the latent heat[2,3] and the magnetization jumps[4–6] indicate the transition order identical to the predicted one. A simple picture of a thermally agitated Abrikosov crystal, however, breaks down when the additional effects of disorder are taken into account. A solid involved in the transition should be then considered as one of the putative phases of a vortex glass,[7,8] an entangled ''supersolid,''[9] or a Bragg glass.[10] The effect of thermal fluctuations is presumably diversified in these solid phases letting them melt either by a first order transition or continuously.

The existence of a critical point (CP) in the phase diagram of untwinned $YBa_2Cu_3O_{7-\delta}$ (YBCO), which was observed by both resistive[11,12] and magnetic[13,14] methods, proves the relevance of diverse vortex matter phases anticipated.[7–10] Approaching the melting transition in the vortex phase diagram, opposite trends were reported. One is the loss of the out-of-plane coherence induced by pointlike disorder[12] and the other is destruction of the in-plane vortex correlations caused by twinning planes.[15] In spite of the contrasting effects of the different types of defects, it was observed that both the melting line $H_m(T)$ for clean crystals[5,6] and the irreversibility line in twinned crystals[16] could be collapsed into a point when plotted against a variable $H/t^{2\nu}$ using the 3D *XY* scaling exponent $\nu=0.669$ for the reduced temperature $t=1-T/T_c$.[17] In most of the discussions of 3D *XY* scaling in oxygen deficient samples,[16,18] the possibility of the change of the order of transition with deoxygenation was ignored. Thus the influence of defects on the order of transition and/or the applicability of 3D *XY* scaling remains unclear.

In this work, we investigate the order of the vortex phase transition as well as the behavior of CP in essentially twin-free YBCO systematically, changing the amount of pointlike disorder and anisotropy by varying the oxygen content. It was found that the first order melting transition can be realized only for $7-\delta>6.94$ in fields up to 7 T applied along *c* axis. For $6.86<7-\delta<6.94$, where the CP crosses our field range ($0 \leqslant H \leqslant 7$ *T*), 3D *XY* scaling cannot well describe the melting line and magnetization data, while for higher and lower oxygen contents the 3D *XY* scaling is applicable.

II. EXPERIMENTS

The single crystals of YBCO were grown by the method of Czochralski,[19] using $3N$-Y_2O_3 crucibles. The crystal growth rate was about 0.01 cm/h. Since the temperature gradient above the surface of the melt was less than 2 °C/cm, the cooling rate of grown crystals was less than 0.02 °C/h. This method gives large (typically 1 cm^3) and pure crystals (99.9%) when flux contamination is carefully avoided. The samples were cut from the large as-grown crystals of high purity and were detwinned by annealing under uniaxial pressure in controlled atomosphere.[20] A small amount of remaining twins with a volume of less than 5% was detected by a neutron diffraction measurement. These pieces were used for

study of different doping states since our method of high-temperature detwinning allowed us to modify oxygen content after detwinning without any retwinning. The oxygen content was controlled by the temperature of post-annealing (from 320 to 550 °C) in oxygen, followed by quenching. Evaluation of oxygen content was based on the scales of Lindemer *et al.*[21] and Yamaguchi *et al.*,[22] which coincide within $\Delta\delta = 0.05$. In this study, we specify the oxygen content by the scale of Ref. 21.

All the data presented here were taken for the 41 mg crystal with dimensions $6 \times 1.4 \times 0.9\,\mathrm{mm}^3 (L_a \times L_b \times L_c)$. This sample showed T_c of 93.5 K in the optimally annealed state. Similar data were obtained on three other high-purity crystals. For a systematic study of oxygen content dependence of the melting phenomenon, it is essentially important to collect all the data on one sample. It allows us in discussion of the change with oxygen content to ignore the other factors such as impurities, defects, sample dimensions and shapes, which can influence magnetization in some cases. In the first set of experiments, when the annealing temperature was increased from experiment to experiment, the sample was annealed for 2–3 weeks at each step. In the second set of experiments, the annealing time was about one week or even shorter and the temperature was reduced step by step. Both sets of experiments gave almost the same T_c values and melting lines. Not only from the sharp superconducting transition observed in small magnetic fields but also from the sharp melting transition in large fields, it was evidenced that the oxygen content was uniform over the sample.

Using the temperature sweep (T-sweep) mode available for Quantum Design SQUID magnetometer (MPMS-XL) we could measure the field-cooled cooling-warming cycles (FCC-FCW) with a dense temperature-field mesh. These precise measurements and the large size of crystals enabled us to gain a sensitivity sufficient to resolve details in magnetization related to the order of the vortex transformation.

III. RESULTS AND DISCUSSIONS

Figure 1 shows the magnetization of field-cooled cooling (FCC) and warming (FCW) with a rate of 0.8 K/min for the slightly underdoped (''$O_{6.86}$'') and the overdoped (''$O_{6.99}$'') crystals. The values of T_c are 93 K for ''$O_{6.86}$'' and 87 K for ''$O_{6.99}$.'' This figure reveals the difference in the order of the vortex melting transformation between the two samples. We find several signatures of the first order transition for ''$O_{6.99}$.'' First, the transition in ''$O_{6.99}$'' is observed as an ''abrupt'' jump which occurs within a few tens of mK, while the transition in ''$O_{6.86}$'' is depicted by the smooth ''continuous'' sigmoidal curve with a width Γ of a few K. The second noticeable feature in ''$O_{6.99}$,'' where the hysteresis in the M-H loops is very small ($J_c \approx 0$), as shown in the inset, is a pronounced hysteresis in the rather rapid FCC-FCW cycles. By contrast, almost no hysteresis is observed in $M(T)$ for ''$O_{6.86}$'' which shows a large J_c in M-H loop. The hysteresis in M-T curve observed only for the ''abrupt'' transition in ''$O_{6.99}$'' is crucial to recognize the coexistence of the solid and liquid phases, which leads to the appearance of a current sheet between these phases because of different flux densities. The interphase currents are flowing in opposite direction to the screening current associated with reversible magnetization M_{rev}. The opposite directed local moments associated with the screening and the bordersheet currents would produce the octupole global contribution seen in the SQUID measurements.[23] Thirdly, the magnitudes of the jumps in ''$O_{6.99}$'' are smaller than those in ''$O_{6.86}$,'' suggesting a plastic phase in the latter sample and a solid/liquid mixture in the former below the transition. Moreover, the following features in Fig. 1 support the first order transition in ''$O_{6.99}$.'' Below an ''abrupt'' jump ΔM_j in the M-H curve for ''$O_{6.99}$,'' corresponding to the jump in M-T curve, critical current density J_c is almost zero in the inset of Fig. 1(a), while for ''$O_{6.86}$,'' a large J_c due to the fishtail effect sets in immediately below the gradual transformation [Fig. 1(b)].

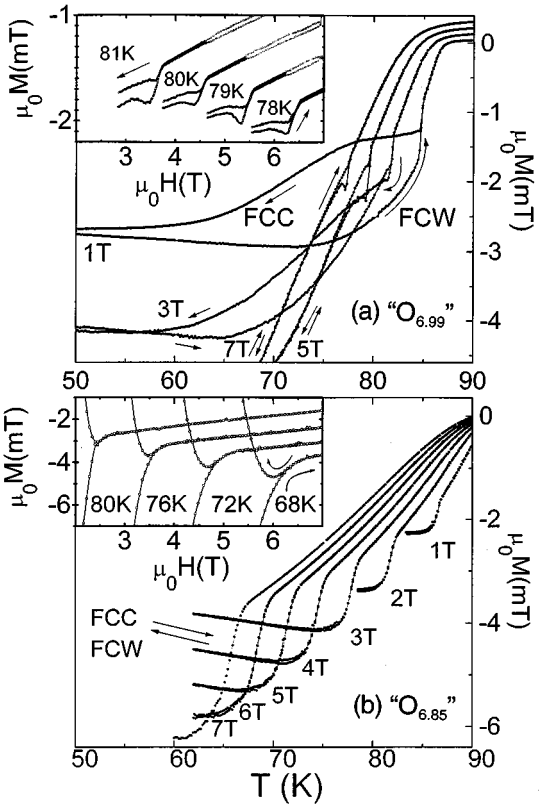

FIG. 1. FC magnetization during cooling (FCC) and warming (FCW) for the crystal of $YBa_2Cu_3O_{7-\delta}$ with the two typical oxygen contents: (a) overdoped ''$O_{6.99}$;'' (b) underdoped ''$O_{6.86}$.'' The T-sweep rate is 0.8 K/min. The insets show the M-H loops near the transition.

Another piece of evidence for the first order transition in ''$O_{6.99}$'' is a discrepancy between the melting temperature T_m and the freezing temperature T_f. When the T-sweep rate is small, we observe that T_m exceeds T_f in ''$O_{6.99}$,'' illustrating undercooling of the vortex liquid, while $T_m = T_f$ in ''$O_{6.86}$.'' A clear discrepancy $\Delta T (= T_m - T_f) \sim 0.1$ K is shown for the measurements with a small sweeping rate of 0.15 K/min in Fig. 2. More detailed results are reported in separate papers.[23,24]

The distinctive features of the first order transition, such as the narrow widths Γ, the negligible pinning $J_c \approx 0$, and FCC-FCW loops were observed only in the region $7-\delta \geqslant 6.94$. We fit our results with the 3D XY scaling law $H_m(T) = H^*(1 - T/T_c^*)^{1.338}$, where both H^* and T_c^* are fitting parameters. In Fig. 3(a), the results of the two-parameter

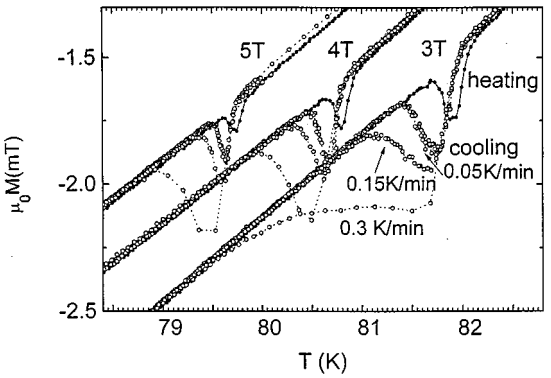

FIG. 2. Temperature dependence of magnetization on in-field cooling and warming with a small T-sweep rate at different magnetic fields. Solid and open circles are the data for warming and cooling, respectively. The cooling rate is changed from 0.05 K/min to 0.3 K/min, while the warming rate is 0.15 K/min.

fit are plotted in coordinates of $H_m^{1/2\nu}$ vs T. It was observed that for $7-\delta>6.92$, the fitted T_c^* values coincide with T_c measured in a small field (10 Oe) within the range of $3\Delta T_c$ [see Fig. 3(b)]. The slopes of melting lines H^* observed in the region $7-\delta>6.9$ are in agreement with the previously reported values from 69.5 to 139 T.[3,5,6,16,17]

The central result of our study is the observation of a crossover from a first order to a second order transition as the oxygen deficiency increases. This is shown in Fig. 3(b) as an abrupt drop near the optimal doping in the $(7-\delta)$ dependence of H^* which correlates with the increase of Γ measured in the T-sweep mode at 7 T. Outside the region $6.86<7-\delta<6.94$, one observes the coincidence of T_c^* and T_c, which underlines the conclusion that the melting lines are well described by the 3D XY power law. In the intermediate δ region (see samples 510, 515, and 520 °C), where the deviation of T_c^* from the measured T_c is pronounced, magnetization jumps are not observed close to T_c but only start from the CP at intermediate fields (1–3 T), and grow with increasing field. The fact that the melting lines in this region are convex indicates the change in slope of $H_m(T)$ from the slope for the first order to that for the second order.

Strictly speaking, the 3D XY model is valid for a transition in zero field. However, as we applied it to the melting transition, and as several researchers suggested,[16–18] an actual range of the critical regime is expected to be rather wide in the magnetic phase diagram. In Fig. 4, the 3D XY scaling is examined in the irreversible region near T_c underneath the melting line, using the variable $H/t^{4/3}$ and $M/t^{4/3}$. In ''$O_{6.99}$,'' for high $T(>70\,\mathrm{K}=0.80T_c)$, the scaling is successful between $H=0$ and H_m. On the other hand, when the measured T range is below the CP temperature, as is seen in ''$O_{6.86}$'' and ''$O_{6.89}$,'' fishtail curves cannot be scaled by the 3D XY law. We also confirmed that the plots of $M/H^{0.5}$ vs $H/t^{2\nu}$ were well scaled by the 3D XY model, as in Refs. 16 and 17, except for the case with the CP in the scaling range.

Figure 4 demonstrates that the 3D XY scaling with $T_c^*=T_c$ does not fit the data near the CP. In the samples ''$O_{6.86}$'' and ''$O_{6.99}$,'' which are far from the CP region, the collapse of melting line into a point is obtained for the parameter T_c^* close to the actual T_c. On the other hand, the

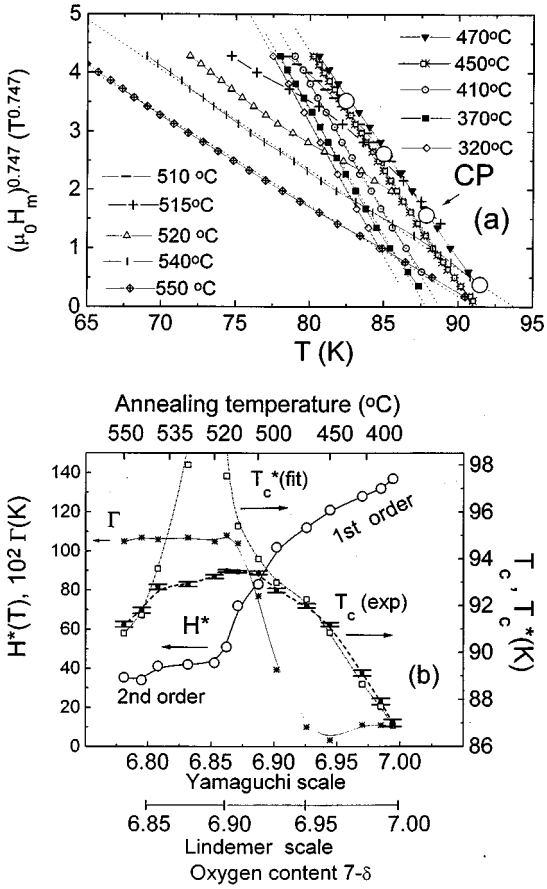

FIG. 3. (a) Melting lines in the single crystal of $YBa_2Cu_3O_{7-\delta}$ annealed in oxygen flow at various temperatures (symbols). The dotted lines are the linear fits, where the cutoffs are the fitted T_c^*'s, and the slopes are $-(H^*)^{0.747}/T_c$. The large open circles show the CP for ''$O_{6.91}$''(510 °C), ''$O_{6.9}$''(515 °C), ''$O_{6.89}$''(520 °C), and ''$O_{6.86}$''(540 °C). (b) Obtained best fit parameters H^* (circles) and T_c^* (open squares) for the melting lines $H_m(T)=H^*(1-T/T_c^*)^{1.338}$ and the transition width Γ (stars) in the fits of FCW data at 7 T near the jump to $M=M_0+M_1T/T_0+\Delta M_J/(1+e^{2(T-Tm)/T})$. The transition at T_m from 10% to 90% of ΔM_J corresponds to 2.1Γ. The filled squares represent experimentally measured T_c's in field of 10 Oe. The error bars show the transition width ΔT_c in susceptibility from 10% to 90% of $1/4\pi$.

scaling with $T_c^*\approx T_c$ is not successful for ''$O_{6.89}$'' in which the melting line is convex. For scaling the melting line above CP, we have to set deliberately $T_c^*=107$ K, as is seen in Fig. 4(b).

It should be noted that M-H loops at the temperatures near the CP indicate a double-peak structure of the fishtail. An example is seen for ''$O_{6.89}$'' in Fig. 4, while more systematic study was reported previously.[20,14] If the origin of the fishtail is associated with the melting phenomenon, the split fishtails in this transient region are consistent with the two characteristic slopes of the melting line in Fig. 3(a). In other words, this may be the evidence for some relationship between the melting phenomenon and the fishtail effect. Note that even in our overdoped samples with a clear transition of the 1st order we have resolved a tiny ''premelting'' peak which is located very close to the melting line ($\approx 0.95H_m$) [see the inset of Fig. 1(a)]. Also in Fig. 4, al-

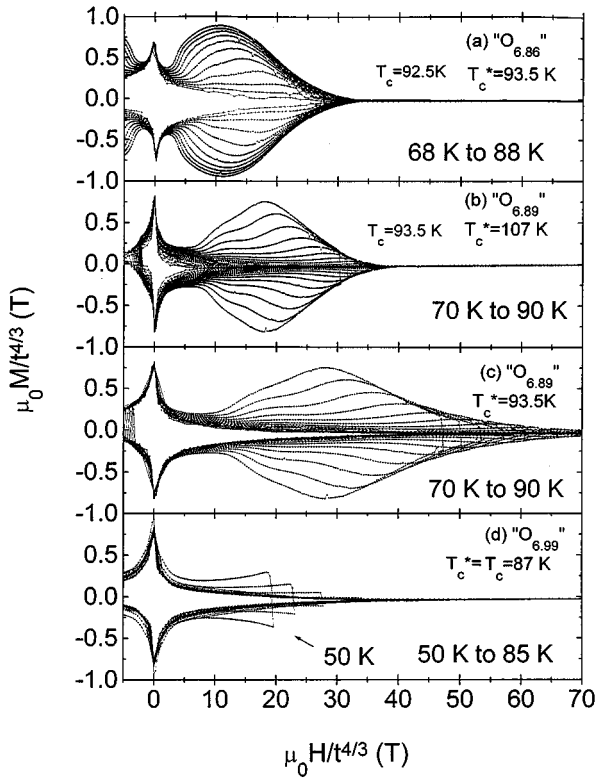

FIG. 4. Magnetization hysteresis loops in the sample ''$O_{6.86}$'' (a), ''$O_{6.89}$'' (b), (c), and ''$O_{6.99}$'' (d). A T interval of the curves is 2 K for (a), (b), and (c), while it is 5 K for (d). Scaling of the zero-field peak widths occurs simultaneously with the 3D XY scaling of the melting line, except for the sample ''$O_{6.89}$'' in which the separate scaling is shown for T_m above CP (b) and for the zero-field peak width (c). T_c^* is an adjustable parameter to collapse into a point of the high-field (above the CP) line of the second order transition.

though a fishtail effect seems to disappear at higher oxygen contents, the observed tail at low temperatures [e.g., 50 K in Fig. 4(d)] suggests the existence of a fishtail at very high field below the melting point (at $H/t^{4/3}=136$ T for ''$O_{6.99}$''). At approaching the CP, where the fishtail line join the melting line, the ''premelting'' peak start to interfere with the fishtail, giving rise to the split fishtail.

It is of great interest in Fig. 4 that within the T range near T_c ($T>0.8T_c$), the zero-field peaks are also scaled by the 3D XY model with the same parameters as for the melting point. For the width of the central peak $H_0(T)$, a scaling parameter $\mu_0 H_0^*=0.6$ T, such that $H_0(T)=H_0^* t^{2\nu}$, can be introduced. Since the field dependence of J_c near zero-field peak is well described by the exponential model[25] as $J_c=J_c(0,T)e^{-H/H_0(T)}$, the data in Fig. 4 can be presented as $J_c(H,T)=J_c(0,0)t^{2\nu}e^{-H/(H_0^* t^{2\nu})}$ with $\mu_0 H_0^*=0.6$ T. Comparing Figs. 4(b) and 4(c), it is concluded that the origin of scaling for the zero-field peak lies at the real value of T_c, which is different from T_c^* determined by fitting in the high field region of the melting line. The known mechanisms of the zero-field peak involve intrinsic pinning[26] and pinning via electromagnetic energy of the vortex lattice.[27] The observed scaling within the 3D XY model for the field H_0 may indicate the existence of a universal fluctuation mechanism underlying both the low-field irreversible behavior and the melting transition. Since a driving force of the scaling in the conventional XY model is a generation of vortex loops, the present result might imply that the vortex loops play an important role for the mechanism of the zero-field pinning as well.

The failure of the 3D XY scaling originates from the convex melting line $H_m(T)$ for the intermediate oxygen contents. If the melting line $H_m(T)$ scales with $H_{c2}(T)$ line, namely, $H_m(T)=CH_{c2}(T)$, C being a constant, as expected in the 3D XY model,[16] then the sharp drop in H^* at $7-\delta=6.94$ can be attributed either to a drop in $C(\delta)$ or to an abrupt change in the slope of $H_{c2}(T)$ at the CP in the vortex phase diagram. The latter case is unlikely, because the zero-field peak width H_0, which shows the same critical exponent as that for $H_{c2}(=H_{c2}^* t^{2\nu})$, exhibits no peculiar feature near the temperature of CP in Fig. 4. In the former case, the slope of the low-field branch of the melting line can be represented as $H^*=C_1 H_{c2}^*$ and $H^*=C_2 H_{c2}^*$ for the first order and second order transitions, respectively. The abrupt change from C_1 to C_2 which results in a dramatic change of H^* implies that the strength of thermal fluctuations required to melt the vortex system is different in elastic and plastic regimes.

A large change in the superconducting condensation energy for small oxygen deficiencies was also reported by Loram *et al.* from the specific heat measurement.[28] They attributed this change to opening of a pseudogap which is characteristic to the underdoped state in high-T_c superconductors. This dramatic decrease in the condensation energy, which must affect H^*,[29] however, is a smooth change between $7-\delta=6.8$ and 6.9, while the change of H^* is steplike in the narrow range of oxygen content around 6.9. Therefore, the jump in H^* in Fig. 3 should be predominantly ascribed to the change in thermal fluctuation strength rather than the change in the condensation energy, as is mentioned above.

Figure 5(a) summarizes the magnitudes of the jumps $\mu_0\Delta M_J$ for various δ and H without making a distinction between the narrow ''discontinuous'' and the broad ''continuous'' jumps. The magnetization jumps ΔM_J are determined by extrapolating the FCW magnetization linearly and measuring the jump as a gap at T_m between the low-T and high-T behaviors. The dashed line represents a trajectory of the CP, which divides the first and the second order transition regions. The magnitude of the jumps for the second order transition increases steadily with the departure from the vicinity of the CP. This behavior can be attributed to increasing plasticity if the jump is coupled with the plastic creep of dislocations at freezing through the second order transition.

On the other hand, in the region of the first order transition, a more complicated behavior is seen. We propose the following explanation, assuming that ΔM_J is affected by the zero-field pinning which increases monotonously with decreasing field toward the zero-field peak $J_c(0)$. At large fields, $J_c\approx 0$ and the slope of FCW magnetization below T_m closely follows that of reversible magnetization $M_{\rm rev}$ above T_m. In the intermediate field range, the slope of $dM_{\rm FCW}/dT$ below T_m decreases because the pinning slows down the relaxation of the excess of negative magnetization, associated with coexistence of solid and liquid phases. This gives an effective increase of ΔM_J at the intermediate fields where

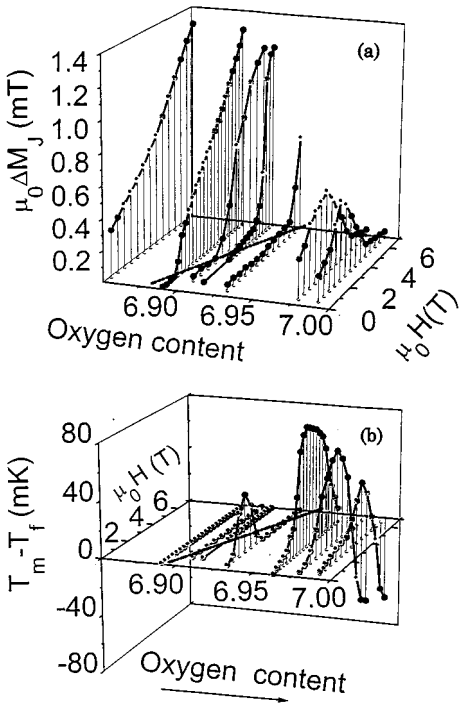

FIG. 5. 3D plot for the magnetization jump ΔM_J (a) and the temperature difference $\Delta T = T_m - T_f$ (b) as a function of oxygen content and magnetic field. The T-sweep rate is 0.05 K/min. The trajectory of the CP is shown by the dashed line.

the value of ΔM_J exceeds by 1–2 orders of magnitude the one expected from the vortex disordering entropy $\Delta S \sim k_B$. On the other hand, at smaller fields, where $dM_{\mathrm{FCW}}/dT \approx 0$, further increase of pinning might start to suppress the phase separation, resulting in a decrease of ΔM_J. Therefore, the coexistence of vortex crystallites with liquid manifests itself most evidently at the intermediate fields.

A similar tendency is observed in the undercooling phenomenon. In Fig. 5(b), the hysteresis in the transition temperature $\Delta T = T_m - T_f$ is plotted against magnetic field and oxygen content. Here also, the dashed line is the trajectory of the CP. As mentioned above, in the region of second order transition, there is almost no hysteresis in M-T curve and thus $\Delta T = 0$. In order to quantify undercooling of the liquid in the first order transition, we define T_m and T_f as the temperatures where $M_{\mathrm{FCW}}(T_m) = M_{\mathrm{rev}} - k\Delta M_J$ and $M_{\mathrm{FCC}}(T_f) = M_{\mathrm{rev}} - k\Delta M_{\mathrm{FCC}}$ with $k = 0.1$. Increase of ΔT with reducing field can be attributed to the delay of crystal nucleation due to decreasing plasticity. (A negative values of ΔT at high fields is merely a consequence of the definition, because in the high field region $\Delta M_{\mathrm{FCC}} \gg \Delta M_J$ and the choice of k value becomes crucial. In fact, if we define T_m and T_f with $k = 0.5$, ΔT does not become negative. The observed feature at high fields shows that the freezing starts at higher temperature but terminates at lower temperature than the melting.) When a field further decreases, ΔT turns to decrease, presumably because of the same reason as that for the decrease in ΔM_J, namely, increase of pinning. As a result, the vortex liquid undercooling is observable on the $H_m(T)$ line in the intermediate field region, where both the delay of vortex crystal nucleation and the liquid-solid separation are most pronounced.

IV. CONCLUSION

We have systematically studied the nature of vortex phase transition in untwinned YBCO single crystals by varying the oxygen contents. In magnetization measurements, depending on the oxygen content and magnetic field, the first order and the second order phase transitions were clearly distinguished by the transition widths, the magnitudes of jumps, the hysteresis in the field-cooled cooling-warming cycles and the superheating of vortex crystallite phenomenon. It was found that the order of transition changes abruptly from the first to the second one near the optimal doping. Since in the crossover region the slope of the melting line changes at the CP, the whole melting line cannot be described as a single line in which H_{c2} is suppressed by the thermal fluctuations, leading to the breakdown of the 3D XY scaling. It means that the nature of thermal fluctuation effect on the melting transition changes between the regions of the first order and the second order, despite the 3D XY scaling is applicable for each region separately.

ACKNOWLEDGMENT

This work was supported by New Energy and Industrial Technology Development Organization (NEDO) for the R&D of Industrial Science and Technology Frontier Program.

[1] E. Brezin, D. R. Nelson, and A. Thiaville, Phys. Rev. B **31**, 7124 (1985).
[2] A. Schilling, R. A. Fisher, N. E. Phyillips, U. Welp, W. K. Kwok, and G. W. Crabtree, Phys. Rev. Lett. **78**, 4833 (1997).
[3] A. Junod, M. Roulin, J.-Y. Genoud, B. Revaz, A. Erb, and E. Walker, Physica C **275**, 245 (1997).
[4] E. Zeldov, D. Majer, M. Konczykowski, V. B. Geshkebein, V. M. Vinokur, and H. Shtrikman, Nature (London) **375**, 373 (1995).
[5] U. Welp, J. A. Fendrich, W. K. Kwok, G. W. Crabtree, and B. W. Veal, Phys. Rev. Lett. **76**, 4809 (1996).
[6] R. Liang, D. A. Bonn, and W. N. Hardy, Phys. Rev. Lett. **76**, 835 (1996).
[7] D. S. Fisher, M. P. A. Fisher, and D. A. Huse, Phys. Rev. B **43**, 130 (1991).
[8] G. Blatter, M. V. Feigelan, V. B. Geshkenbein, A. I. Larkin, and V. M. Vinokur, Rev. Mod. Phys. **66**, 1125 (1994).
[9] E. Frey, D. R. Nelson, and D. S. Fisher, Phys. Rev. B **49**, 9723 (1994).
[10] T. Giamarchi and P. Le Doussal, Phys. Rev. B **52**, 1242 (1995).
[11] H. Safar, P. L. Gammel, D. A. Huse, D. J. Bishop, W. C. Lee, J. Giapintzakis, and D. M. Ginsberg, Phys. Rev. Lett. **70**, 3800 (1993).
[12] D. Lopez, L. Krusin-Elbaum, H. Safer, E. Righi, F. de la Cruz, S. Grigera, C. Field, W. K. Kwok, L. Paulius, and G. W. Crabtree,

Phys. Rev. Lett. **80**, 1070 (1998).
[13] T. Nishizaki, T. Naito, and N. Kobayashi, Physica C **282-287**, 2117 (1997).
[14] K. Deligiannis, P. A. J. de Groot, M. Oussena, S. Pinfold, R. Langan, R. Cargnon, and L. Taillefer, Phys. Rev. Lett. **79**, 2121 (1997).
[15] D. Lopez, E. F. Righi, G. Nieva, and F. de la Cruz, Phys. Rev. Lett. **76**, 4034 (1996).
[16] J. R. Cooper, J. W. Loram, J. D. Johnson, J. W. Hodby, and C. Changkang, Phys. Rev. Lett. **79**, 1730 (1997).
[17] M. B. Salamon, J. Shi, N. Overend, and M. A. Howson, Phys. Rev. B **47**, 5520 (1993).
[18] M. A. Hubbard, M. B. Salamon, and B. W. Veal, Physica C **259**, 309 (1996).
[19] J. Czochralski, Z. Phys. Chem., Stoechiom. Verwandtschaftsl. **92**, 219 (1917); Y. Yamada and Y. Shiohara, Physica C **217**, 182 (1993).
[20] A. I. Rykov, W. J. Jang, H. Unoki, and S. Tajima, in *Advances in Superconductivity VIII*, edited by H. Hayakawa and Y. Enomoto (Springer-Verlag, Tokyo, 1996), p. 341.
[21] T. B. Lindemer, J. F. Hunley, J. E. Gates, A. L. Sutton, J. Brynestad, and C. R. Hubbard, J. Am. Ceram. Soc. **72**, 1775 (1989).
[22] S. Yamaguchi, K. Terabe, A. Saito, S. Yahagi, and Y. Iguchi, Jpn. J. Appl. Phys., Part 2 **27**, L179 (1988).
[23] A. I. Rykov, Physica C **297**, 133 (1998).
[24] A. I. Rykov and S. Tajima, in *Advances in Superconductivity X*, edited by K. Osamura and I. Hirabayashi (Springer-Verlag, Tokyo, 1998), p. 83.
[25] T. Kobayashi, T. Kimura, J. Shimoyama, K. Kishio, K. Kitazawa, and K. Yamafuji, Physica C **254**, 213 (1995).
[26] L. W. Conner, A. P. Malozemoff, and I. A. Campbell, Phys. Rev. B **44**, 403 (1991).
[27] S. Senoussi, C. Aguillon, and P. Manuel, Physica C **175**, 20 (1991).
[28] J. W. Loram, K. A. Mirza, J. R. Cooper, W. Y. Liang, and J. M. Wade, J. Supercond. **7**, 243 (1994).
[29] We also estimated $H^* = 4$ T for $7-\delta = 6.6$ (Ref. 20), which is an order of magnitude smaller than the values for $7-\delta > 6.85$ just as is similar to the specific heat jump in Ref. 28.